Reentrant Interface Depinning from Rough Walls[1]

G. Giugliarelli[2, 3] and A. L. Stella[4]

Depinning of an interface from a rough self-affine wall delimiting an attractive substrate is described in terms of directed paths on a square lattice. Short range interactions are assumed and the phase diagram is determined by transfer matrix methods for several values of ζ_w, the roughness exponent of the wall. For all ζ_w the following scenario is observed. At a very low temperature T, the interface is not pinned for wall attraction energies below a certain ζ_w-dependent, nonzero threshold. This contrasts with the case of smooth walls, for which the threshold is zero. In a range of attraction energies just below the threshold, a pinning transition first occurs, as T increases, followed by a depinning one (reentrant depinning). This unusual reentrance phenomenon, in which, upon increasing T, dewetting is followed by wetting, is peculiar of self-affine roughness and does not occur, e.g., with a periodic substrate corrugation. The nature of both wetting and dewetting transitions is determined by the value of ζ_w. As found in related work, the two transitions are both continuous or both first-order, according to whether $\zeta_w < 1/2$, or $\zeta_w > 1/2$, respectively. The border value $\zeta_0 = 1/2$ coincides with the intrinsic roughness of the interface in the bulk.

KEY WORDS: geometrical surface disorder; phase diagram; statistical physics; wetting.

1. INTRODUCTION

The properties of an interface are strongly influenced by the presence of a substrate. In wetting phenomena, for example, the interface between two coexisting phases unbinds from an attractive substrate (wetting transition) as the temperature is increased [1]. While wetting is rather well understood

---

in pure systems, the effects of disorder [2–5] are still actively investigated. Of particular interest is the case of geometric surface disorder (roughness) and its effects on location and nature of wetting transitions [2].

Here we focus our attention on some effects of self-affine roughness on the wetting phase diagram. Self-affine roughness is often encountered in experimental samples [6]. Self-affinity implies that the average (transverse) height fluctuation of a sample of (longitudinal) linear size X, ΔW_X, scales like $\Delta W_X \sim X^{\zeta_W}$. The role of this kind of roughness in both complete and critical wetting phenomena has been investigated by several methods in recent years [7, 8]. Most recently it was found [9, 10] that self-affine roughness changes critical wetting transitions into first-order when the substrate roughness, ζ_W, exceeds the roughness of the interface in the bulk, ζ_0. This is expected to hold for both ordered and disordered bulks and with short-range substrate forces. As we show here, this change of transition order is not the only effect of surface roughness on interface properties. Self-affine roughness radically modifies the wetting phase diagram in a way which can be important in experiments and applications [11].

In the present paper we study the wetting phase diagram of a generalization with rough wall [9] of a standard interfacial model with short range forces in 2D [12]. Our results give evidence of some remarkable and unusual features of the phase diagram, which, at a qualitative level, should be considered as generic for wetting on self-affine rough substrates. The most notable feature of the phase diagram is a reentrant interface depinning in the whole range of roughnesses $(0 < \zeta_W < 1)$. This reentrance, which amounts to a dewetting followed by a wetting transition as the temperature is raised, occurs both in regimes when the transitions are continuous, and when they are first-order.

This paper is organized as follows. In the next section we introduce the model and describe our transfer matrix method. In Section 3 we discuss the main results for the phase diagram. In Section 4 further general considerations and conclusions are given.

2. THE MODEL

Let us consider a 2D square lattice and denote by x and y the integer coordinates of its sites. Self-avoiding paths (partially) directed in the x direction, like that shown in Fig. 1, are considered as possible interface configurations. Because of the directed nature of the paths, a particular configuration is determined by giving the ordinate $y = h_x$ of the left-hand extremity of each one of its horizontal steps. We suppose that the substrate wall is also represented by a directed path defined in terms of a set of step ordinates $\{W_x\}$ defined in the same way as $\{h_x\}$. The impenetrable character
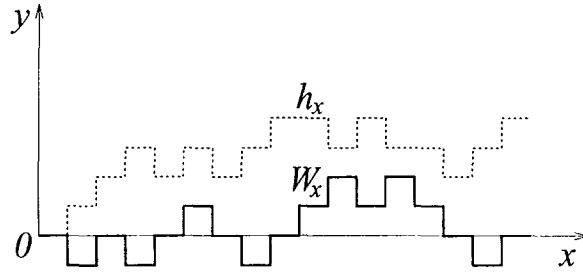
Fig. 1.   Example of a rough substrate wall (continuous path) and
an interface configuration (dotted path).

of the wall implies obviously that $h_x \geqslant W_x$. Moreover, we impose the
following restrictions on the sets $\{h_x\}$ and $\{W_x\}$: (a) $h_{x+1} - h_x = 0, \pm 1$;
(b) $W_{x+1} - W_x = \pm 1$. Such restrictions are imposed merely for computa-
tional convenience; removing or modifying them would not change the
main qualitative features of our results.

The sets $\{W_x\}$ are randomly generated by an iterative algorithm [11,
13]. This algorithm produces directed paths in 2D obeying the restrictions
described above and the scaling relation,

$$\overline{|W_{x+\Delta x} - W_x|} \sim |\Delta x|^{\varsigma_w} \tag{1}$$

In this equation and in the following, the overbars indicate quenched
averages over samples of $\{W_x\}$.

To each interface configuration with a projection of length X on the
x axis is associated an energy E_x,

$$E_X = \sum_x^X \left[\mathscr{E}(1 + |z_x - z_{x-1} + w_x|) - U\delta_{z_x, 0} \right] \tag{2}$$

where $z_x = h_x - W_x$ and $w_x = W_x - W_{x-1}$. In Eq. (2) $\mathscr{E}$ $(\mathscr{E} > 0)$ is the
energy cost of each interface step and $-U$ $(U > 0)$ is the energy gain of an
interface contact with the attracting wall. Only the horizontal steps of the
interface paths in contact with the wall are assigned the energy $-U$; this
is a particular feature of our model. This choice is not mandatory, and dif-
ferent conventions would not change the basic qualitative results.

At a finite temperature T the properties of the interface can be studied
in terms of the partition function,

$$\mathscr{Z}_X = \sum_{\{z_x\}} e^{-(E_X/k_B T)} = \omega^X \sum_{\{z_x\}} \omega^{n_\perp} k^{n_c} \tag{3}$$

where $\omega = e^{-\mathscr{E}/k_{\mathrm{B}}T}$ and $k = e^{U/k_{\mathrm{B}}T}$ are the fugacities associated with each (horizontal or vertical) step of the path and each horizontal step on the wall, respectively. The sum is done over the ensemble of all the directed paths (determined here by $\{z_x\}$) compatible with the chosen profile of the wall. $n_{\perp}$ and n_c are the number of vertical steps of the interfacial path and the number of its horizontal steps on the wall, respectively.

The interface partition depends on the temperature T and the energies U and $\mathscr{E}$ through the dimensionless parameters $u = U/\mathscr{E}$ and $t = k_{\mathrm{B}}T/\mathscr{E}$. We refer to u and t as wall attraction strength and temperature, respectively.

Making use of the transfer matrices $\mathbf{T}_{w_x}$ defined as follows,

$$(\mathbf{T}_w)_{m,n} = [\delta_{m,n-w} + \omega(\delta_{m,n-w-1} + \delta_{m,n-w+1})] \, k^{\delta_{m,0}}, \qquad w = \pm 1 \qquad (4)$$

the partition function in Eq. (3) can be expressed as

$$\mathscr{Z}_X = \omega^X \sum_{l,z} \left(\prod_{x=1}^{X} T_{w_x} \right)_{l,z} \cdot \phi_0(z) \qquad (5)$$

The function ϕ_0 establishes particular $x = 0$ conditions for the interfacial paths. For example, for paths with the left extremity on the wall, we put $\phi_0(z) = \delta_{z,0}$.

A wall profile corresponds to a particular sequence of factors $\mathbf{T}_{w_x}$ in the product of Eq. (5). For asymptotically large systems $(X \to \infty)$, the partition function $\mathscr{Z}_X$ can be expressed in terms of the largest Lyapunov eigenvalue $\lambda_{\max}$ [14] of the matrix product in Eq. (5) as $\mathscr{Z}_X \sim (\omega\lambda_{\max})^X$. Useful tools for the numerical calculation of $\lambda_{\max}$ are the normalized vectors $\vec{\psi}_x$ defined by the recursion relation,

$$\vec{\psi}_x = \frac{1}{n_x} \mathbf{T}_{w_x} \vec{\psi}_{x-1} \qquad (6)$$

with $\|\vec{\psi}_x\| = \sum_z \psi_x(z)$, $n_x = \|\mathbf{T}_{w_x}\vec{\psi}_{x-1}\|$ and $\vec{\psi}_0 \equiv \vec{\phi}_0$. Because of the particular normalization rule, it is simple to see that the zth component of the vector $\vec{\psi}_x$ corresponds to the probability that the path at x is at a distance z from the wall [2, 8]. This interpretation of $\vec{\psi}_x$ guides our choice of $\|\vec{\psi}_x\|$. For a given wall profile, the above definitions allow to express the Lyapunov eigenvalue $\lambda_{\max}$ as

$$\lambda_{\max} = \lim_{X \to \infty} \left[\prod_{x=1}^{X} n_x \right]^{1/X} = \exp\left(\lim_{X \to \infty} \frac{1}{X} \sum_{x=1}^{X} \ln n_x \right) \qquad (7)$$

Finally, we can consider the quenched dimensionless free energy density, $\bar{f}$, given by $\bar{f} = -\lim_{X \to \infty} \overline{\ln \mathcal{Z}_X}/X$. With the last definitions this can be written as

$$\bar{f} = -\overline{\ln \omega \lambda_{max}} = -\ln \omega - \lim_{X \to \infty} \overline{\frac{1}{X} \sum_{x=1}^{X} \ln n_x} \tag{8}$$

3. WETTING PHASE DIAGRAM

The depinning transition occurs because, e.g., at a fixed temperature, the interface remains bound to the wall only for sufficiently high values of u. In the case of a flat wall, i.e., $\{W_x = \text{constant } \forall x\}$, the value of u, u_c, above which the interface is pinned has been calculated exactly [15, 12, 2]. The exact formulas can be used to write the wall critical attraction strength, at which the interface depinning takes place, in the form,

$$u_c(t) = t \ln[(1 + 2 \exp(-1/t))/(1 + \exp(-1/t))] \tag{9}$$

from which one can see that $\lim_{t \to 0} u_c(t) = 0$. On the other hand, if we denote by P_0 the average fraction of horizontal interface steps on the wall, $P_0 = \lim_{X \to \infty} \langle n_c \rangle / X$, with brackets indicating canonical thermal average; from the same formulas one can see that P_0 vanishes continuously and linearly in $u - u_c$ when the line $u = u_c(t)$ is approached from above.

When dealing with random walls, the calculation of f or P_0 for each particular $\{W_x\}$ can be done only numerically. To minimize finite size effects due to truncations of the transfer matrices, in our calculations we always considered matrix sizes much larger than the mean square perpendicular width of the self-affine walls. In practice we used transfer matrices as large as $10^4 \times 10^4$ in the roughest case, corresponding to $\zeta_W = \ln 12/\ln 32 \simeq 0.717$. With this roughness $X = 10^5$ was reached. In addition, one has to average over different $\{W_x\}$ in order to get $\bar{f}$ and $\overline{P_0}$. We could sample at most 10 or 15 $\{W_x\}$ in the most favorable cases, due to the large X's needed to extract precisely f and P_0.

At fixed t, as the transition is approached from above [viz., $u > u_c(t)$], the interface free energy density [Eq. (8)] is negative and increasing, with decreasing u; at $u = u_c(t)$ it matches the bulk interface free energy density $f_{bulk} = -\ln \omega(1 + 2\omega)$. Thus, the depinning transition can be located where the interface excess free energy $\Delta f = f - f_{bulk}$ vanishes. The calculation of $\overline{P_0}$ offers an alternative way of locating the transition, by identifying the conditions under which this quantity first becomes zero.

Once the free energy f and P_0 had been obtained for a sufficient number of wall profiles, we evaluated both $\bar{f}$ and $\overline{P_0}$. We could observe that

both quantities can be used to locate the transition with approximately the same precision. A careful numerical study of how $\overline{P_0}$ or Δf approach zero gave us further information on whether the transition is continuous or first-order [9].

Figure 2 summarizes the results we have obtained by a systematic calculation of $\bar{f}$ as a function of t and u, for five values of ζ_W. The curves in the figure represent the behavior of u_c versus t. u_c was determined numerically as the value of u below which $|\Delta f| \leq 0.0001$ as u was changed in steps of 0.001.

Looking at the transition curves for rough walls in Fig. 2, we note two main differences from the flat case.

(a)   For all ζ_W, $u_c(t)$ is positive and finite. As $t \to 0$ the minimal attraction strength needed to pin an interface, $u_c(0)$, is finite and increases as the wall roughness ζ_W increases.
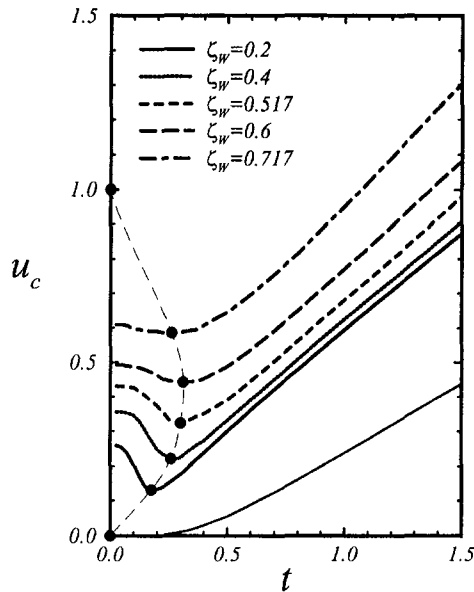
Fig. 2. Interface phase diagram for rough self-affine walls in the t–u plane. The curves $u = u_c(t)$ are shown for five values of the roughness exponent ζ_W. The light continuous line corresponds to $u = u_c(t)$ for a flat wall as given by Eq. (9). The light dashed line gives a qualitative idea of the dependence of t_R on ζ_W.

(b) All the curves $u = u_c(t)$ present a minimum at t_R. As a consequence, there is a temperature interval in which u_c is a decreasing function of t.

The minimum in the transition lines is responsible for a remarkable reentrance effect. In fact, let us focus our attention on one of the $u = u_c(t)$ lines in Fig. 2. As in an experiment, the interface behavior can be monitored at fixed u, by varying t. We identify three regimes

(1) For $u < u_c(t_R)$ interface pinning is impossible, no matter how low t is.

(2) For $u_c(t_R) < u < u_c(0)$ as the temperature is increased, the interface undergoes two transitions: (i) at an effective temperature $t_D < t_R$, we find an unexpected pinning transition—the substrate is wet for $t < t_D$ and dewets at $t = t_D$; and (ii) at some $t_W > t_R$ a more usual depinning (wetting) transition follows.

(3) For $u > u_c(0)$ as the temperature is increased, the interface passes from a pinned to a depinned state at some t_W.

A detailed study of the behavior of t_R for ζ_W approaching zero is not feasible due to the necessity of generating extremely long walls in order to distinguish very low from strictly zero roughness. The same calculations for ζ_W approaching 1 are again very time-consuming mainly because of the large dimension of the transfer matrices required to avoid finite size effects. However, our results suggest rather clearly that t_R approaches zero for both $\zeta_W \to 0$ and $\zeta_W \to 1$. Thus, in these two limits the reentrance disappears. In Fig. 2 we draw a line which joins the points $(t_R, u(t_R))$ of our curves with $(0, 0)$ and $(0, 1)$. This line should give a qualitative idea of the dependence of t_R on ζ_W.

Another interesting aspect of the phase diagram is that connected to the nature of the transitions involved. The continuous or discontinuous character of the wetting transitions upon varying ζ_W was discussed in Ref. 9 by analyzing the way in which $\overline{P_0}$ approaches zero for $u \to u_c(t)^+$. While in this work we focus our attention mainly on the wetting phase diagram, we made also a study of the nature of the reentrant dewetting transition for two ζ_W values, respectively, below and above $\zeta_W = 1/2$. In the first case ($\zeta_W = 0.4$) we found evidence of a continuous depinning, while in the latter ($\zeta_W = 0.6$) it appeared discontinuous. These results are in agreement with those of Ref. 9 for wetting transitions, and suggest that also for dewetting $\zeta_W = 1/2$ could be the border line roughness between continuous and discontinuous depinning.

4. CONCLUSIONS

The results presented in the previous section are worth discussing further.

At $t = 0$, in order to decide whether the interface is pinned or not, we need only to compare the ground state energy in the bulk with the lowest energy of a state in which the interface is bound to the substrate. In the bulk, the state of lowest possible energy is clearly given by a straight configuration ($n_\perp = 0$). A bound state will have an energy relative to this unbound ground state equal to $\delta n_\perp - U n_c \cdot n_\perp$ and n_c depend, of course, on the wall configuration to which this bound state refers. Clearly $u_c(0)$ is determined by the condition under which this energy difference between the two states vanishes: $u_c(0) = \lim_{X \to \infty} n_\perp/n_c$. The fact that bound ground state configurations satisfy this limit condition with $u_c(0) > 0$ is a nontrivial property of self-affine substrates. On a periodically corrugated substrate with average horizontal slope, this limit property would not be satisfied. In this case, for u very close to zero, the bound ground state configuration is one in which $n_\perp = 0$, corresponding to a straight interface touching the attractive tips of the periodically corrugated wall. Thus, we would have $n_\perp = 0$ and $n_c \neq 0$, and, consequently, $u_c(0) = 0$, as in a flat case. We conclude that a remarkable property of self-affine substrates is that they can support ground state interface configurations with $\lim_{X \to \infty} n_\perp/n_c > 0$.

We also verified, by explicit calculations for simple periodically corrugated walls, that u_c is always an increasing function of t, contrary to what happens in the self-affine case. Indeed, a remarkable property of self-affine substrates, for which $u_c(0) > 0$ is clearly a necessary but not sufficient condition, is the monotonically decreasing character of the curve $u = u_c(t)$ in the interval $(0, t_R)$. This feature implies that, as soon as t rises above zero, an interface can be more easily bound to the rough substrate. This clearly shows that there is a very nontrivial energy–entropy interplay in the pinning mechanism when self-affine roughness is involved.

The calculations we presented in this work have been limited to 2D and to strictly short range forces. For the moment the extension of these calculations to 3D is computationally unfeasible, and even the inclusion of long-range potentials would pose serious additional difficulties in our calculations. However, in 3D we expect that the main features of the phase diagram would persist. Concerning the effect of long-range forces, which should certainly be included in more realistic calculations to compare with experiments, we can only conjecture that they would not modify the main result obtained here, i.e., the reentrance. However, there is at least one experimental system, namely interfaces in superconductors [16], for which a short-range description should be fully adequate.

REFERENCES

1. For a wide review on wetting phenomena, see S. Dietrich, in *Phase Transitions and Critical Phenomena*, Vol. 12, C. Domb and J. L. Lebowitz, eds. (Academic Press, London, 1988).
2. G. Forgacs, R. Lipowsky, and Th. M. Nieuwenhuizen, in *Phase Transitions and Critical Phenomena*, Vol. 14, C. Domb and J. L. Lebowitz, eds. (Academic Press, London, 1991).
3. D. A. Huse and C. L. Henley, *Phys. Rev. Lett.* **54**:2708 (1985).
4. M. Kardar, *Phys. Rev. Lett.* **55**:2235 (1985); M. Kardar and D. R. Nelson, *Phys. Rev. Lett.* **55**:1157 (1985).
5. R. Lipowski and M. E. Fisher, *Phys. Rev. Lett.* **56**:472 (1986).
6. P. Pfeifer, Y. J. Wu, M. W. Cole, and J. Krim, *Phys. Rev. Lett.* **62**: 1997 (1989); see also J. Krim, I. Heyvaert, C. Van Haesendonck, and Y. Bruynseraede, *Phys. Rev. Lett.* **70**:57 (1993).
7. H. Li and M. Kardar, *Phys. Rev. B* **42**:6546 (1990); M. Kardar and J. O. Indekeu, *Europhys. Lett.* **12**:61 (1990).
8. G. Giugliarelli and A. L. Stella, *Physica A* **212**:12 (1994).
9. G. Giugliarelli and A. L. Stella, *Phys. Rev. E* **53**:5035 (1996).
10. G. Sartoni, A. L. Stella, G. Giugliarelli, and M. R. D'Orsogna, *Europhys. Lett.* **39**:633 (1997).
11. G. Giugliarelli and A. L. Stella, *Physica A* **239**:467 (1997).
12. S. T. Chui and J. D. Weeks, *Phys. Rev. B* **23**:2438 (1981).
13. B. B. Mandelbrot, *Phys. Scripta* **32**:257 (1985).
14. A. Crisanti, G. Paladin and A. Vulpiani, in *Products of Random Matrices in Statistical Physics*, H. K. Lotsch, ed., Springer Series ill Solid State Sciences, Vol. 104 (Springer, Berlin, 1993).
15. D. Abraham, *Phys. Rev. Lett.* **44**:1165 (1980).
16. J. O. Indekeu and J. M. J. van Leeuwen, *Phys. Rev. Lett.* **75**:1618 (1995).